Layer-number dependent high-frequency vibration modes in few-layer transition metal dichalcogenides induced by interlayer couplings*

Qing-Hai Tan[1,2], Xin Zhang[1], Xiang-Dong Luo[1,3], Jun Zhang[1,2], and Ping-Heng Tan[1,2,†]

[1]State Key Laboratory of Superlattices and Microstructures, Institute of Semiconductors, Chinese Academy of Sciences, Beijing 100083, China
[2]College of Materials Science and Opto-Electronic Technology, University of Chinese Academy of Sciences, Beijing 100049, China
[3]Jiangsu Key Laboratory of ASIC Design, Nantong University, Nantong 226007, China

Abstract: Two-dimensional transition metal dichalcogenides (TMDs) have attracted extensive attention due to their many novel properties. The atoms within each layer in two-dimensional TMDs are joined together by covalent bonds, while van der Waals interactions combine the layers together. This makes its lattice dynamics layer-number dependent. The evolutions of ultralow frequency (< 50 cm^{-1}) modes, such as shear and layer-breathing modes have been well-established. Here, we review the layer-number dependent high-frequency (> 50 cm^{-1}) vibration modes in few-layer TMDs and demonstrate how the interlayer coupling leads to the splitting of high-frequency vibration modes, known as Davydov splitting. Such Davydov splitting can be well described by a van der Waals model, which directly links the splitting with the interlayer coupling. Our review expands the understanding on the effect of interlayer coupling on the high-frequency vibration modes in TMDs and other two-dimensional materials.

Key words: transition metal dichalcogenides; Raman spectroscopy; interlayer coupling; Davydov splitting; van der Waals model

DOI: 10.1088/1674-4926/38/3/031006 **PACS:** 63.22.Np; 71.35.Gg; 78.30.-j

1. Introduction

Bulk transition metal dichalcogenides (TMDs) MX_2 (e.g., M = Mo or W, X = S, Se or Te) have a layered structure, similar to bulk graphite. In MX_2, each unit layer contains three atomic layers in which one M atom is sandwiched between two X atoms. MX_2 have many novel physical properties. Generally, MX_2 show an indirect to direct band gap evolution from bulk to monolayer[1,2]. The valley polarization degree in MX_2 can be manipulated optically or electronically, which makes MX_2 have huge potential applications in valley electronics[3]. Specially, two MX_2 flakes can be easily formed into van der Waals (vdW) heterostructures[4–6] in which the lattice mismatch effect is ignorable. The novel properties of MX_2 have attracted extensive attention and MX_2 have been applied to various optoelectronic devices[7,8]. As a layered material, the adjacent layers of bulk MX_2 are bounded by the weak vdW interaction, which allows its exfoliation into multilayer and monolayer. The physical properties of MX_2 flakes are strongly dependent on the weak interlayer coupling. The Raman spectroscopy is a useful tool to nondestructively probe the physical properties in layered materials, such as the crystal structure[9,10], stacking order[11–13], lattice vibrations and interlayer coupling[10,14]. In particular, Raman spectroscopy can be used to probe the interlayer coupling and identify the layer number of layered materials, such as graphene, MX_2 and alloy flakes[15–18].

The Raman spectrum of bulk and multilayer (ML) MX_2 consists of two fundamentally different sets of Raman peaks. Those peaks, such as $A_1'/A_{1g}^2/A_{1g}$ and $E'/E_g^1/E_{2g}^1$, etc, present also in monolayer MX_2, due to in-plane or out-of-plane vibrations, but the shear (S) modes and layer breathing (LB) modes (LBMs), due to relative motions between different layers, only present in multilayer cases. The crystal lattices of even N layers (ENL), odd N layers (ONL) and bulk MX_2 have different symmetries and thus the modes with similar atomic displacements are assigned by specific denotations, such as A_1'/E' in ONL MX_2, A_{1g}^2/E_g^1 in ENL MX_2 and A_{1g}/E_{2g}^1 in bulk MX_2. In general, each Raman mode in 1L MX_2 will split into N corresponding Raman modes in NL MX_2. It is clear that the acoustic modes in 1L MX_2 will evolve into the S and LB modes in NL MX_2. The S and LB frequencies are diverged from that of the acoustic modes, which is resulted from the interlayer coupling due to the out-of-phase vibrations between two adjacent X atom layers in NL MX_2. It is the same case for the optical modes in 1L MX_2. For a layered crystal with 2 layers per unit cell, the frequency difference between the in-phase and out-of-phase vibrations of the two equivalent entities is well-known as Davydov splitting, as discussed in bulk As_2S_3, As_2Se_3[19] and β-GaSe[20]. In general, for NL MX_2, each layer vibration gives rise to a set of N near-degenerate vibration modes due to the weak interlayer coupling.

In this review, we will discuss the Davydov splitting and interlayer coupling in NL MX_2, and then introduce a simple

* Project supported by the National Basic Research Program of China (No. 2016YFA0301200), the National Natural Science Foundation of China (Nos. 11225421, 11474277, 11434010, 61474067, 11604326, 11574305 and 51527901), and the National Young 1000 Talent Plan of China.

† Corresponding author. Email: phtan@semi.ac.cn

Received 8 November 2016, revised manuscript received 30 December 2016

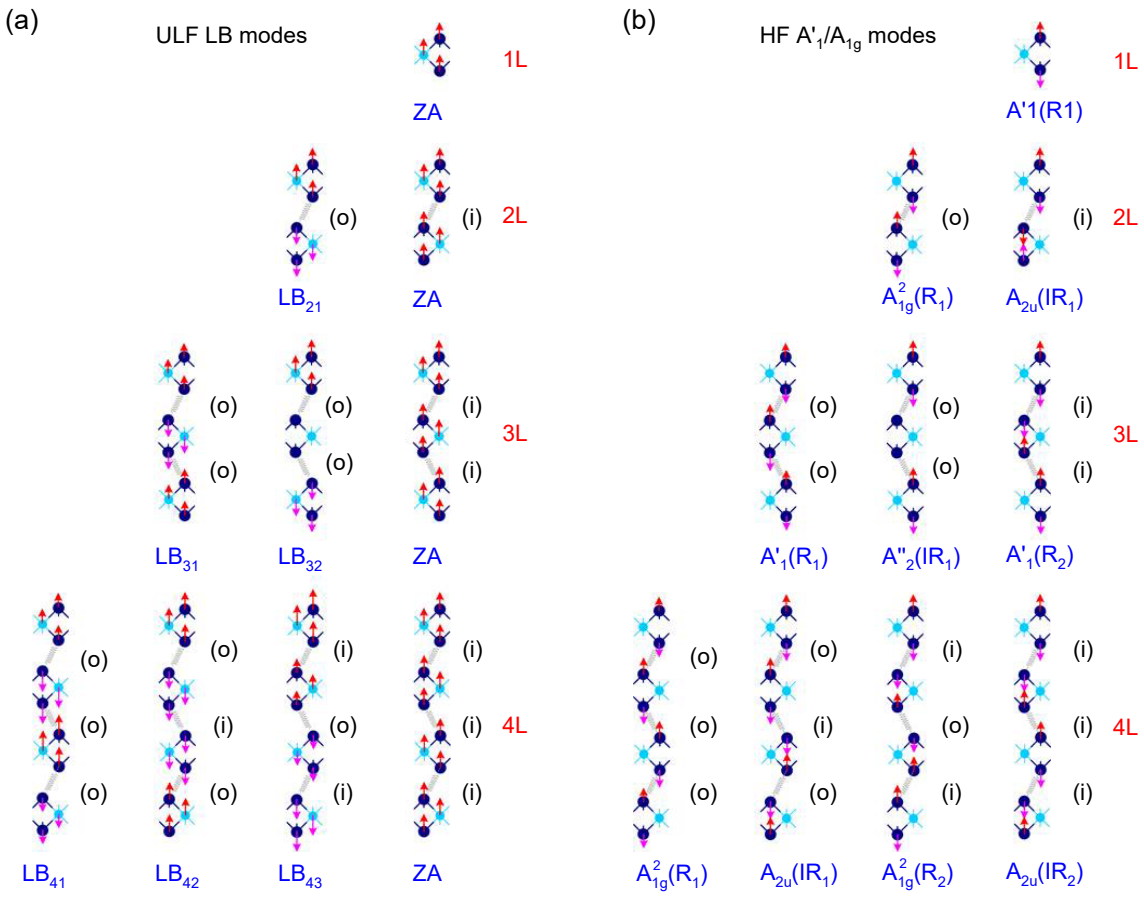

Fig. 1. (Color online) (a) The atoms displacements of (a) layer breathing (LB) modes and (b) A_1'-like modes in 1-4L MX_2. (o) and (i) represent that two X atoms in adjacent layers vibrate out-of-phase and in-phase, respectively.

vdW model to bridge the frequency between interlayer S/LB modes and the high-frequency optical modes derived from the corresponding modes in 1L MX_2. Based on the vdW model, the mode frequency of the high-frequency optical modes in NL MX_2 can be directly estimated by the frequency of the S and LB modes in NL MX_2 and the corresponding optical modes in 1L MX_2.

2. Lattice vibrations of MX_2

Lattice vibrations of NL MX_2 can be denoted by the irreducible representations of the factor group of crystals. For bulk 2H MX_2, the unit cell is composed of six atoms belonging to D_{6h} point group. There are 18 normal vibrational modes at the Γ point[10, 14]: $\Gamma = A_{1g} + 2A_{2u} + 2B_{2g} + B_{1u} + E_{1g} + 2E_{1u} + 2E_{2g} + E_{2u}$, where A_{1g}, E_{1g} and E_{2g} are Raman (R) active, one A_{2u} and one E_{1u} are acoustic, another A_{2u} and E_{1u} are infrared (IR) active, and B_{2g}, B_{1u} and E_{2u} are optically silent. The unit cells of bulk and bilayer (2L) MX_2 are the same, but the unit cell of 2L MX_2 belongs to D_{3d}. There are 18 normal vibrational modes at the Γ point[10, 14]: $\Gamma = 3A_{1g} + 3A_{2u} + 3E_g + 3E_u$, where one A_{2u} and one E_u are acoustic modes, the other A_{2u} and E_u are IR active, and A_{1g} and E_g are R active. The monolayer (1L) has a D_{3h} point group and the irreducible representations are shown as[10, 14]: $\Gamma = 2A_2'' + A_1' + 2E' + E''$, where one A''(ZA) and one E' are acoustic modes, another A_2'' is IR active, A' and E'' are R active and another E' is both R and IR active. For 2L MX_2, the unit cell is composed of six atoms belonging to D_{3d}. Each of the nine normal vibrational modes in 1L MX_2 will split into the corresponding two modes in both 2L and bulk MX_2, where the displacement of the adjacent X atom layers between two X–M–X layers is in-phase for one mode and out-of-phase for another mode. The additional "spring" coupling from out-of-phase vibration increases the frequency of E_g^1 and E_{2g}^1 with respect to E_u/E_{1u}. This is known as "Davydov splitting", which also occurs to other modes in 2L and bulk MX_2.

For NL MX_2, each mode in 1L MX_2 will split into near-degenerate vibration modes. Here we take the A_1' mode in 1L MX_2 as an example to explain this splitting. Because ENL MX_2 and ONL MX_2 have D_{3d} and D_{3h} point groups, respectively, the A_1' mode in 1L MX_2 can be expressed as $\frac{N+1}{2}A_1' + \frac{N-1}{2}A_2''$ for ONL MX_2 and $\frac{N}{2}A_{2u} + \frac{N}{2}A_{1g}^2$ for ENL MX_2, where the A_1' and A_{1g}^2 modes are Raman active and the A_2'' and A_{2u} modes are infrared active. Here we simply named those Raman modes as A_1'-like. To identify Raman modes with the same notation, we use R_i and IR_i to assign the i^{th} Raman active and infrared active modes, respectively. The N Raman modes exhibit atomic displacements with a different number of out-of-phase or in-phase displacements between X atoms of neighboring layers. We present the atomic displacements of $A_1'(A_{1g})$ and LB modes of 1–4L MX_2, as shown in Fig. 1. Such atomic displacements can be calculated by the diatomic chain model[15, 16]. If we take A_1'-like modes in 4L MX_2 as an exam-

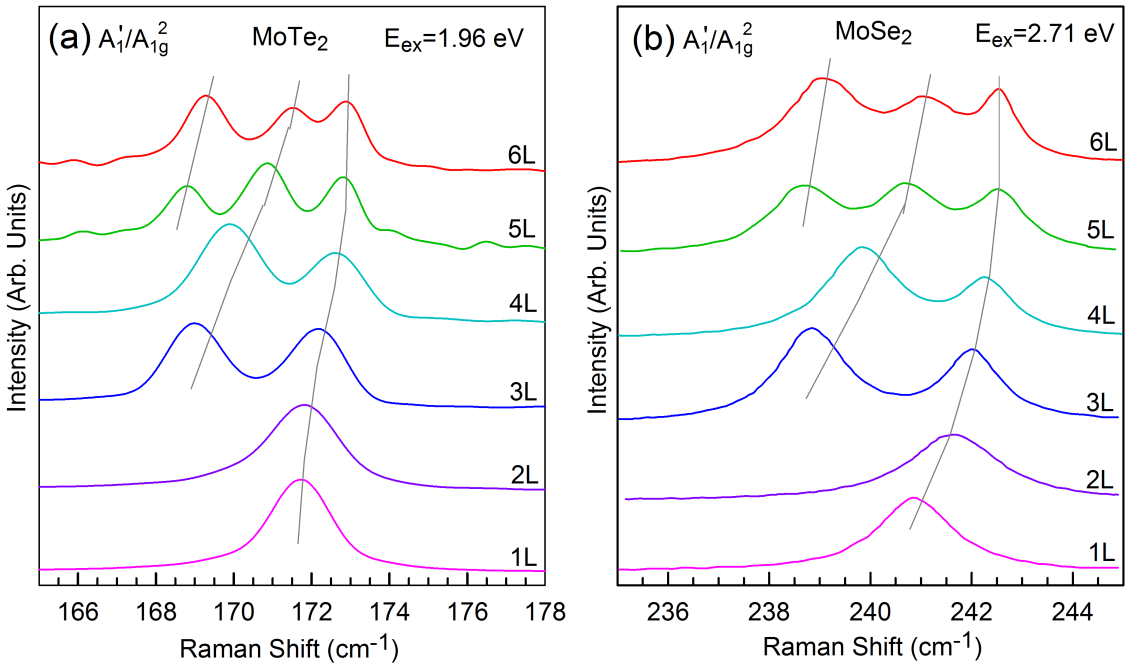

Fig. 2. (Color online) Raman spectra of A_1'-like modes in 1–6L (a) $MoTe_2$ flakes[21] and (b) $MoSe_2$ flakes[22].

ple, the $A_{1g}^2(R_1)$, $A_{2u}(IR_1)$, $A_{1g}^2(R_2)$ and $A_{2u}(IR_2)$ modes have 3, 2, 1 and 0 out-of-phase displacements between X atoms of neighboring layers, respectively. The atomic displacements of A_1'-like modes in NL MX_2 are out of plane, while those of the LB modes and out-of-plane acoustic (ZA) modes are also out of plane. The LB_{41}, LB_{42}, LB_{43} and ZA modes also have 3, 2, 1 and 0 out-of-phase displacements between X atoms of neighboring layers, respectively. For each optical mode in 1L MX_2, its corresponding optical modes in NL MX_2 have the similarity as the S or LB modes on the number of out-of-phase displacements between X atoms of neighboring layers, dependent on whether the atomic displacements are in-plane or out-of-plane. The interlayer couplings in MX_2 completely determine the frequencies of all the S and LB modes, and the frequency splitting can be as large as tens of wavenumbers. Thus, the frequency splitting is expected between any two A_1'-like modes in NL MX_2 that are derived from the A_1' mode in 1L MX_2. It is also expected for other sets of Raman modes in NL MX_2.

3. Experimental observation of Davydov splitting in few-layer MX_2

In fact, the general Davydov splitting is known as the splitting of bands in the electronic or vibrational spectra of crystals due to the presence of more than one (interacting) equivalent molecular entity in the unit cell[21]. Indeed, three and four equivalent entities can be found in many systems and the corresponding Davydov components have been observed. Thus, the concept of Davydov splitting related with bulk and 2L MX_2 can be extended to NL MX_2 ($N > 2$), for which there exist N equivalent entities in its unit cell for Davydov splitting. Each equivalent (isolated) entity is an M atom sandwiched by two X atoms in the unit cell of 1L MX_2. The mode corresponds to the uncoupled entities in which all the nearest X atoms in adjacent layers vibrate in phase, e.g., the $A_1(R_2)$ mode in 3L MX_2 and the $A_{2u}(IR_2)$ mode in 4L MX_2. The other $N-1$ modes correspond to the $N-1$ coupled entities in which at least one pair of nearest X atoms in adjacent layers vibrates out of phase. The out-of-phase vibrations between nearest X atoms in adjacent layers of the coupled entities will result in a frequency different from the uncoupled entities, and Davydov components are formed in NL MX_2. Therefore, each optical mode in 1L MX_2 can correspond to N corresponding Davydov components in NL MX_2 ($N > 1$), which can be directly observed by Raman spectroscopy once at least two Davydov components are Raman active. Based on the symmetry analysis for bulk and 2L MX_2[10,14], only one of the Davydov doublets can possibly be Raman active, and thus it is difficult to observe the Davydov doublets just by Raman spectroscopy in bulk and 2L MX_2[19,20,23,24]. That is why it is necessary to measure both Raman and infrared spectra to reveal Davydov splitting in bulk materials.

With increasing N, more modes are Raman active. It is thus possible to observe the Davydov splitting in NL MX_2 just by Raman spectroscopy[21,22,25,27]. The Davydov splitting of A_1'-like modes in 2–6L $MoTe_2$ and $MoSe_2$ are depicted in Figs. 2(a) and 2(b), respectively. It is obvious that the number of Davydov components is layer-number dependent. The number of the observed Raman modes is equal to that of Raman active A_1'/A_{1g}^2 modes in NL MX_2. The previous reports[21,22,26,27] indicate that proper excitation energy is necessary to observe the Davydov components in NL MX_2. The frequency and total number of Davydov components in NL MX_2 can be used as a simple way to identify the layer number of MX_2 flakes[21].

4. vdW model for Davydov splitting in few-layer MX_2

The S and LB modes in layered materials are directly related to their interlayer coupling[14–17]. Since the atomic dis-

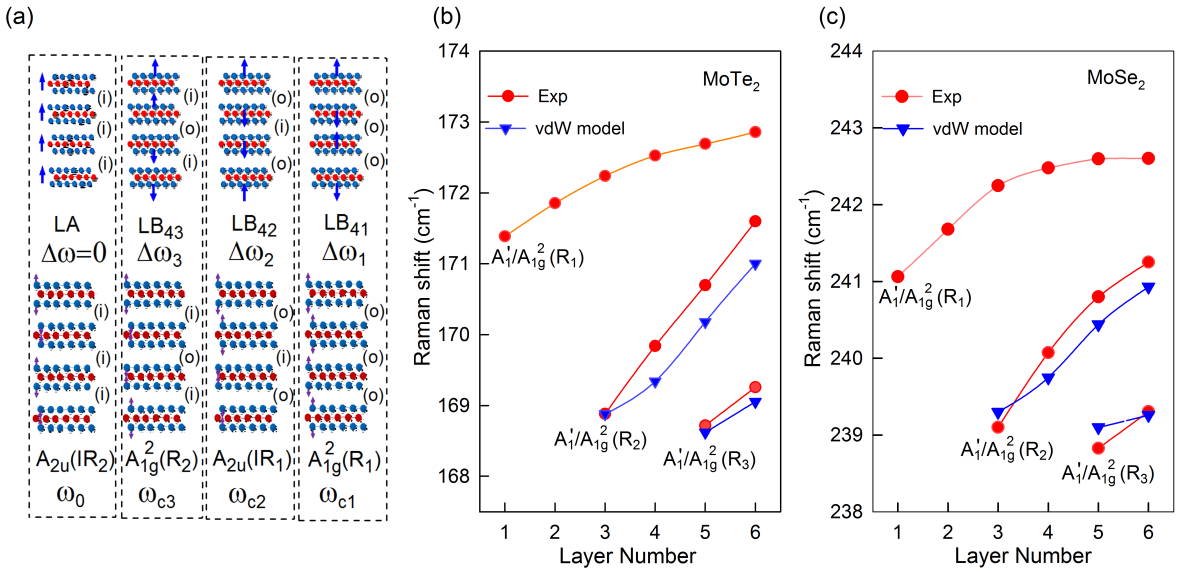

Fig. 3. (Color online) (a) Atomic displacements of LB and A_1'-like modes in 4L MX_2[21]. (b) The experimental (Exp) frequency (solid red circles) and the calculated one based on the vdW model for the A_1'-like modes in 1-6L $MoTe_2$ flakes[21]. (c) The experimental (Exp) frequency (solid red circles) and the calculated one based on the vdW model for the A_1'-like modes in 1-6L $MoSe_2$ flakes[22]. The solid line is a guide for the eye.

placements of A_1'/A_{1g}^2 modes are perpendicular to the basal plane, just like the LB modes, if one only considers the first-order approximation, the frequencies of Davydov components are expected to be closely related to the LB coupling. The frequencies of two Davydov doublets in bulk (or 2L) layered materials[20, 28] follow the relation of $\omega_c^2 = \omega_0^2 + \Delta\omega^2$, where ω_0 is the frequency of the isolated entity or that of two uncoupled entities when the two entities vibrate in phase, ω_c is the frequency of two coupled entities when they vibrate out of phase, and $\Delta\omega$ is the coupling frequency between two coupled entities. This model has been extended to NL MX_2, i.e., $\omega_{cj}^2 = \omega_0^2 + \Delta\omega_j^2$ ($j = 1, 2, \ldots, N-1$), where ω_0 is the frequency of the isolated entity or that of N uncoupled entities when the N entities vibrate in phase, ω_{cj} is the j^{th} frequency of N coupled entities when at least two of them vibrate out of phase, and $\Delta\omega_j$ is the j^{th} coupling frequency of N coupled entities when at least two of them vibrate out of phase. We denote this model as the vdW model because we assume that the interlayer couplings in layered materials are exclusively of the vdW interactions. Because the atomic displacements of the A_1'-like modes are perpendicular to the basal plane, the interlayer LB coupling is responsible for the frequency difference between any two Davydov components. Considering that there exists a counterpart of A_1'-like modes for each LB mode so that both the two modes have the same number of out-of-phase displacements between X atoms of neighboring layers, each LB frequency is the coupling frequency in the vdW model, and the corresponding A_1'-like mode is the N coupled entity. Thus, $\Delta\omega_j = \omega(\text{LB}_{Nj})$. The above model can also be applied to E′-like and E″-like modes in NL MX_2, in which $\Delta\omega_j = \omega(S_{Nj})$. Fig. 3(a) shows the atomic displacements of the LB and A_1'-like modes in 4L MX_2, where four pairs of A_1'-like and LB modes are indicated.

The vdW model can be checked by the frequencies of the observed LB and A_1'-like modes in NL MX_2. All the frequencies of LB_{Ni} can be measured by the ultralow-frequency Raman technique[15, 16]. The frequency of unobserved LB modes can be estimated by the linear chain model[15, 16]. In principle, the frequency of the A_1'-like mode, such as $A_1'(R_2)$ in 3L MX_2 and $A_{2u}(IR_2)$ in 4L MX_2, in which all the nearest X atoms in adjacent layers vibrate in phase, should be equal to that of the A_1' mode in 1L MX_2. Because their mode frequency can also be affected by other factors, such as stacking induced structure changes and long-range Coulombic interlayer interactions, we cannot treat these modes as a standard to calculate other mode frequencies based on the vdW model. Similar to the case of $A_{1g}^2(R_1)$ in 3L MX_2 and $A_{2u}(IR_2)$ in 4L MX_2, the A_1'-like mode in NL MX_2 with $N-1$ out-of-phase displacements between X atoms of neighboring layers are always Raman active and can be observed in Raman spectra. Such a mode is with the highest frequency among the set of Davydov components in NL MX_2. Therefore, we can calculate the Davydov splitting with respect to the mode with the highest frequency. Figs. 3(b) and 3(c) show the measured frequency (red solid circles)[21, 22] of Davydov components in each NL $MoTe_2$ and $MoTe_2$, respectively. The calculated frequency of Davydov components based on the vdW model is depicted in Figs. 3(b) and 3(c) by solid triangles, which is in good agreement with the experimental data.

As discussed above, in principle, the frequency of uncoupled entities in NL MX_2 should be equal to that of the isolated entity in 1L MX_2 because all the nearest X atoms in adjacent layers vibrate in phase. However, it is not the case in both NL $MoTe_2$ and $MoSe_2$ because there may exist long-range Coulombic interlayer interactions in NL $MoTe_2$ and $MoSe_2$, which are dependent on N. Indeed, the frequency difference between the A_1' mode in 1L $MoTe_2$ ($MoSe_2$) and the $A_1'(R_1)$ mode in 5L $MoTe_2$ ($MoSe_2$) is about 2.3–2.6 cm^{-1}. Even so, the Davydov splitting in each NL $MoTe_2$ and $MoSe_2$ can be well understood by the vdW model. This suggests that the frequency difference between Davydov components in NL

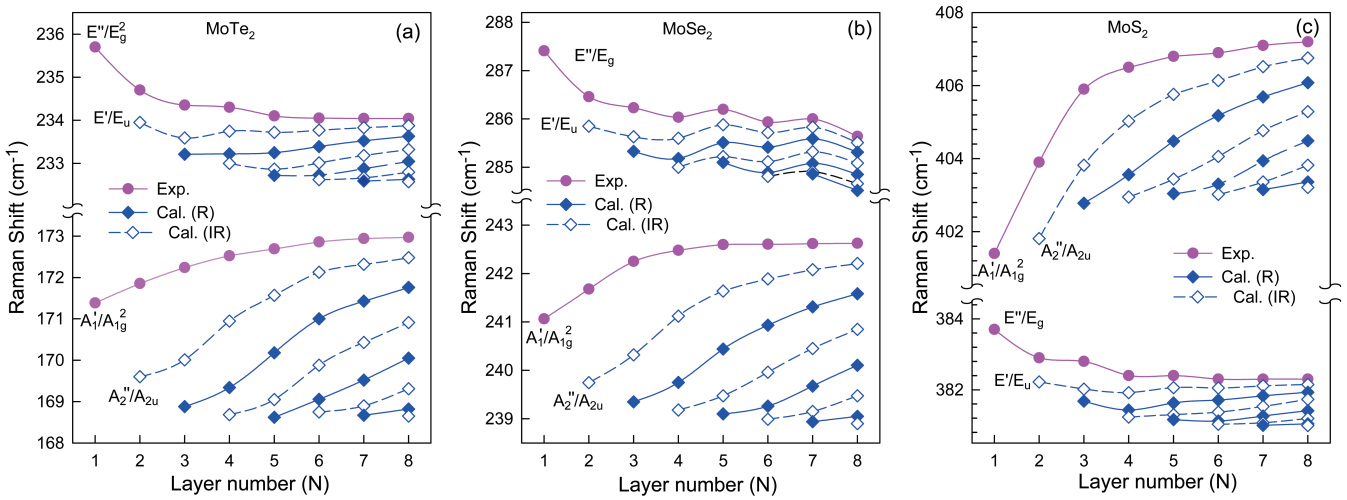

Fig. 4. (Color online) The calculated (Cal.) frequency of each Davydov component for A_1'-like and E″-like modes (blue diamonds) in 1-8L (a) $MoTe_2$, (b) $MoSe_2$ and (c) MoS_2 flakes based on the vdW model. The experimental (Exp.) frequency of the Davydov component with the highest frequency (pink circles) in $MoTe_2$, $MoSe_2$ and MoS_2 flakes is used as a reference frequency for calculation. The Raman-active (R) and infrared-active modes are shown by solid and open diamonds, respectively.

$MoTe_2$ and $MoSe_2$ is mainly determined by the interlayer vdW interactions, which opens the possibility to study the interlayer vdW interactions in other layered materials by Davydov splitting of the high-frequency optical modes.

Because the vdW model links the frequency of the S or LB modes with that of a high-frequency mode, we can estimate the frequency evolution of the high-frequency mode with N based on the vdW model even some modes are Raman inactive and cannot be observed in the experiments. Fig. 4 demonstrates the N-dependent frequency of the E″-like and A_1'-like modes in 1–8L $MoTe_2$, $MoSe_2$ and MoS_2 based on the vdW model. Since the atomic displacements of the E″-like modes are in plane, the coupling frequency is from the corresponding S modes. Because the maximum frequency of the S mode is smaller than that of the LB mode, the maximum Davydov splitting between two in-plane high frequency modes is smaller than that between two out-of-plane high frequency modes. Thus, the Davydov splitting between two specific A_1' modes is much larger than that between two corresponding E″-like modes, no matter that the frequency of the A_1' modes is larger or smaller than that of the E″-like modes. For a given S or LB frequency, the smaller the frequency of the isolated entity is, the larger the Davydov splitting is observed. The evolutions of the S and LB frequencies in NL MX_2 are completely determined by the S and LB frequencies in 2L MX_2 based on the linear chain model. Therefore, once we measured the high-frequency Raman modes of 1L MX_2 and the S and LB modes in 2L MX_2, we can calculate the Davydov splitting of the high-frequency Raman modes of NL MX_2. A model related with multiple force constants has also been proposed to well understand Davydov splitting in NL MX_2[22, 27]. However, it has so many parameters for fitting that make it difficult to qualitatively estimate such Davydov splitting in NL MX_2.

5. Conclusions

In conclusion, we have reviewed lattice vibrations and Davydov splitting in monolayer and few-layer MX_2, such as $MoTe_2$, $MoSe_2$ and MoS_2. It is found that the vdW model can be used to well fit and predict the frequency evolution of Davydov components in NL MX_2, suggesting that the Davydov splitting between two Davydov components in NL MX_2 is mainly determined by the interlayer vdW interactions. This review provides a deeper understanding on the lattice dynamics in two-dimensional TMDs. This model can also be used for twisted multilayer flakes of other two-dimensional materials[29, 30].

References

[1] Splendiani A, Sun L, Zhang Y B, et al. Emerging photoluminescence in monolayer MoS_2. Nano Lett, 2010, 10(16): 1271
[2] Mak K F, Lee C G, Hone J, et al. Atomically thin MoS_2: a new direct-gap semiconductor. Phys Rev Lett, 2010, 105(20): 136805
[3] Cao T, Wang G, Han W P, et al. Alley-selective circular dichroism of monolayer molybdenum disulphide. Nat Commun, 2012, 3(8): 887
[4] Geim A K, Grigorieva I V. Van der Waals heterostructures. Nature, 2013, 499(10): 419
[5] Dean C, Young A F, Wang L, et al. Graphene based heterostructures. Solid State Commun, 2012, 152(6): 1275
[6] Liang L B, Meunier V. First-principles Raman spectra of MoS_2, WS_2 and their heterostructures. Nanoscale, 2014, 6(4): 5394
[7] Lou Z, Liang Z Z, Shen G Z. Photodetectors based on two dimensional materials. J Semicond, 2016, 37(9): 091001
[8] Xia C X, Li J B. Recent advances in optoelectronic properties and applications of two-dimensional metal chalcogenides. J Semicond, 2016, 37(5): 051001
[9] Lee C G, Yan H G, Brus L E, et al. Anomalous lattice vibrations of single-and few-layer MoS_2. ACS Nano, 2010, 4(9): 2695
[10] Zhang X, Qiao X F, Shi W, et al. Phonon and Raman scattering of two-dimensional transition metal dichalcogenides from monolayer, multilayer to bulk material. Chem Soc Rev, 2015, 44(1): 2757
[11] Puretzky A A, Liang L B, Li X F, et al. Low-frequency Ra-

man fingerprints of two-dimensional metal dichalcogenide layer stacking configurations. ACS Nano, 2015, 9(53): 6333

[12] Wu J B, Wang H, Li X L, et al. Raman spectroscopic characterization of stacking configuration and interlayer coupling of twisted multilayer graphene grown by chemical vapor deposition. Carbon, 2016, 110(9): 225

[13] Zhang X, Han W P, Qiao X F, et al. Raman characterization of AB- and ABC-stacked few-layer graphene by interlayer shear modes. Carbon, 2016, 99(10): 118

[14] Zhang X, Tan Q H, Wu J B, et al. Review on the Raman spectroscopy of different types of layered materials. Nanoscale, 2016, 8: 6435

[15] Tan P H, Han W P, Zhao W J, et al. The shear mode of multilayer graphene. Nat Mater, 2012, 11(6): 294

[16] Zhang X, Han W P, Wu J B. et al. Raman spectroscopy of shear and layer breathing modes in multilayer MoS_2. Phys Rev B, 2013, 87(1):115413

[17] Zhao Y Y, Luo X, Li H, et al. Interlayer breathing and shear modes in few-trilayer MoS_2 and WSe_2. Nano Lett, 2013, 13(2): 1007

[18] Qiao X F, Li X L, Zhang X, et al. Substrate-free layer-number identification of two-dimensional materials: a case of $Mo_{0.5}W_{0.5}S_2$ alloy. Appl Phys Lett, 2015, 106(22): 223102

[19] Zallen R, Slade M L, Ward A T. Lattice vibrations and interlayer interactions in crystalline As_2S_3 and As_2Se_3. Phys Rev B, 1971, 3(17): 4257

[20] Wieting T J, Verble J L. Interlayer bonding and the lattice vibrations of β-GaSe. Phys Rev B, 1972, 5(0): 1473

[21] Song Q J, Tan Q H, Zhang X, et al. Physical origin of Davydov splitting and resonant Raman spectroscopy of Davydov components in multilayer $MoTe_2$. Phys Rev B, 2016, 93(9): 115409

[22] Kim K, Lee J U, Nam D, et al. Davydov splitting and excitonic resonance effects in Raman spectra of few-layer $MoSe_2$. ACS Nano, 2016, 10(8): 8113

[23] Verble L, Wieting T J. Lattice mode degeneracy in MoS_2 and other layer compounds. Phys Rev B, 1970, 25(4): 362

[24] Wieting T J, Verble J L. Infrared and Raman studies of long-wavelength optical phonons in hexagonal MoS_2. Phys Rev B, 1971, 3(0): 4286

[25] Tonndorf P, Schmidt R, Philipp B, et al. Photoluminescence emission and Raman response of monolayer MoS_2, $MoSe_2$, and WSe_2. Opt Express, 2013, 21(4): 4908

[26] Staiger M, Gillen R, Scheuschner N, et al. Splitting of monolayer out-of-plane A'_1 Raman mode in few-layer WS_2. Phys Rev B, 2015, 91(8): 195419

[27] Froehlicher G, Lorchat E, Fernique F, et al. Unified description of the optical phonon modes in n-layer $MoTe_2$. Nano Lett, 2015, 15(10): 6481

[28] Ghosh P N, Maiti C R. Interlayer force and Davydov splitting in 2H-MoS_2. Phys Rev B, 1983, 28(3): 2237

[29] Wu J B, Zhang X, Ijaes M, et al. Resonant Raman spectroscopy of twisted multilayer graphene. Nat Commun, 2014, 5(7): 5309

[30] Lin M L, Ran F R, Qiao X F, et al. Ultralow-frequency Raman system down to 10 cm^{-1} with longpass edge filters and its application to the interface coupling in t(2+2) LGs. Rev Sci Instrum, 2016, 87(5): 053122